

## Coating of Ti-6Al-4V Metal Alloys Nanotube with Hydroxyapatite-Gelatin-Polyvinyl Alcohol Composites using the Dip-Coating Methods

Charlena Charlena<sup>1\*</sup>, Setyanto Tri Wahyudi<sup>2</sup>, Cucu Putri Nurmawan<sup>1</sup>

<sup>1</sup>Departemen Kimia IPB University, Kampus Dramaga Bogor, Jl. Agatis Kampus Dramaga Bogor 16680

<sup>2</sup>Departemen Fisika IPB University, Kampus Dramaga Bogor, Jl. Agatis Kampus Dramaga Bogor 16680

\*Corresponding author: [charlena@apps.ipb.ac.id](mailto:charlena@apps.ipb.ac.id)

DOI: <https://doi.org/10.24198/cna.v13.n1.57959>

**Abstract:** The Ti-6Al-4V metal alloy is an implantable material because of its strength, lightweightness, and corrosion resistance properties. Metal alloy surfaces need to be modified to improve corrosion resistance. Therefore, the study aims to modify the surface of Ti-6Al-4V metal alloys to form nanotube structures and to coat the hydroxyapatite composite (HAp)-gelatin-PVA in Ti-6Al-4V metal alloys. Nanotubes were formed by anodizing methods in an ethylene glycol-H<sub>2</sub>O (9:1) solution containing 0.6% NH<sub>4</sub>F at 20V for 3 hours. The result of SEM showed that the diameter of the nanotube hole is about 30–40 nm and that it is formed homogeneously. The result of coating nanotube metal alloys with composite HAp-gelatin-PVA is that they are evenly distributed and thicker. The morphology of a homogeneous small granule composite coating composite. The X-ray diffraction showed shows that the composite HAp-gelatin-PVA crystalline size coated on nanotube metal alloy is smaller than that of non-nanotube. Nanotube Ti-6Al-4V coated metal alloy with HAp-gelatin-PVA composites had shows poor bioactivity that had not beenand thus not able to increase the corrosion resistance of Ti-6Al-4V metal alloys.

**Keywords:** anodization, gelatin, hydroxyapatite, nanotube, Ti-6Al-4V

**Abstrak:** Paduan logam Ti-6Al-4V digunakan sebagai bahan implan karena sifatnya kuat, ringan, dan tahan korosi. Permukaan paduan logam perlu dimodifikasi untuk meningkatkan ketahanan terhadap korosi. Untuk itu, penelitian ini bertujuan memodifikasi permukaan paduan logam Ti-6Al-4V membentuk struktur nanotube serta menyalutkan komposit hidroksiapatit (HAp)-gelatin-PVA pada paduan logam Ti-6Al-4V. Nanotube dibentuk melalui metode anodisasi dalam larutan etilena glikol-H<sub>2</sub>O (9:1) yang mengandung NH<sub>4</sub>F 0.6% pada tegangan 20V selama 3 jam. Hasil pencirian SEM menunjukkan diameter lubang nanotube sekitar 30–40 nm dan terbentuk secara homogen. Hasil penyalutan paduan logam nanotube dengan komposit HAp-gelatin-PVA merata dan lebih tebal. Morfologi komposit penyalut berbentuk granula kecil yang homogen. Pencirian difraksi sinar-X menunjukkan bahwa ukuran kristal komposit HAp-gelatin-PVA yang tersalut pada paduan logam nanotube lebih kecil dibandingkan dengan non nanotube. Nanotube paduan logam Ti-6Al-4V yang tersalut dengan komposit HAp-gelatin-PVA memiliki bioaktivitas yang kurang baik sehingga belum dapat meningkatkan ketahanan korosi paduan logam Ti-6Al-4V.

**Kata kunci:** anodisasi, gelatin, hidroksiapatit, nanotube, Ti-6Al-4V.

### INTRODUCTION

Bone damage, such as fractures or cracks in the bone due to accidents, has increased the need for implant materials. Implants can replace damaged bone so that it can function again. The most commonly used implant material is metal because it has good mechanical properties, is strong, and is easy to mould. Titanium metal and its alloys, such as Ti-6Al-4V, have advantages over other metals, namely high biocompatibility, good corrosion resistance, and mechanical properties such as hardness and good wear resistance (Chen & Thouas 2015). Titanium and its alloys have low bioactive properties (Charlena *et al.* 2018a), so it is necessary to treat the surface. However, the low biocompatibility and bioactivity of

the metal causes corrosion of the metal due to body fluids.

Metal surfaces need to be modified to improve corrosion resistance. Modifications that can be made include heat treatment, anodisation, and thin membrane coating (Shirdar *et al.* 2016). The modification carried out in this study is the formation of nanotube surfaces on metal alloys using anodisation. Anodisation is an electrochemical electroplating process that will make the material form a titanium oxide layer that is not only resistant to corrosion but also has high hardness. The advantages of modification with anodisation are that it is easy to do and produces an oxide layer with a higher hardness value than the parent metal. With this

process, it is expected that the characteristics of the oxide layer produced have high thickness and hardness, and corrosion resistance can be achieved. The corrosion resistance of Ti-6Al-4V nanotubes is lower than that of non-nanotubes, but both are better than that of Ti-6Al-4V without nanotubes. In vitro, bioactivity tests of nanotubes decreased faster than non-nanotubes (Charlena *et al.* 2022). Another thing that can be done to reduce the problems found in metals is to coat the metal with bioceramics.

The bioceramic used is hydroxyapatite (HAp). Metal coating by HAp is a way to improve the biocompatibility of metals. However, HAp alone has the disadvantage of being brittle and unstable when used for bone implants. HAp coated on the metal surface must have a small pore size. The addition of gelatin aims to reduce the pore size. The advantage of HAp with tiny pores is that it expands its surface to reduce the frictional force that occurs with the tissue when applied in the body. HAp-gelatin composite is a suitable alloy to improve resistance to cracking, corrosion, and biocompatibility. The best composite is 30% HAp-gelatin synthesised by the in-situ method because the crystallinity is the highest, and SEM results show smaller and more homogeneous granules (Monica *et al.* 2016). However, the resulting 30% HAp-gelatin composite is still brittle. Adding polyvinyl alcohol (PVA) will effectively improve the uniformity and hardness of the HAp-gelatin composite. This is because PVA has good biocompatibility properties and can interact with gelatin molecules and body tissues due to its hydrophilic nature. The addition of PVA can also reduce the corrosion rate of HAp-chitosan composites coated on Ti-6Al-4V metal because PVA can block the release of metal ions from the surface of Ti-6Al-4V metal (Charlena *et al.* 2022).

The composite will be deposited on the surface of the surface-modified metal using the dip-coating method. The advantages of the dip-coating method include the uniformity of the HAp surface can be adjusted, the time required is fast, and the composite layer is deposited on the metal surface without any reaction or decomposition occurring between the composite and the metal surface (Mohseni *et al.* 2014). This research aims to bond Ti-6Al-4V nanotube metal alloy with HAp-gelatin-PVA composite using the asa method and compare with the bonding of Ti-6Al-4V non-nanotube metal alloy.

## MATERIALS AND METHODS

### Materials

All reagents used in this study were Ti-6Al-4V metal alloy, 96% ethanol, acetone, concentrated nitric acid, ammonium fluoride, ethylene glycol, diammonium hydrogen phosphate, strontium chloride, concentrated ammonium hydroxide, sodium hydroxide, calcium hydroxide, Simulated Body Fluid (SBF), universal pH indicator, gelatin, polyvinyl alcohol (PVA), 0.9%, distilled water, aquabides,

platinum (Pt) electrodes, and Silicon Carbide sandpaper bags.

This study consists of five stages, namely the synthesis of HAp-gelatin-PVA by wet precipitation method in-situ, the formation of nanotubes on the surface of Ti-6Al-4V metal alloy, coating by dip-coating method, corrosion test and in vitro test on SBF solution, and characterisation of the results by atomic absorption spectrophotometer (AAS), X-ray diffraction (XRD), Fourier transform infrared spectrophotometer (FTIR), and Scanning Electron Microscope (SEM).

### Synthesis of HAp-Gelatin-Polyvinyl Alcohol by In-Situ Wet Precipitation Method (Monica *et al.* 2016)

$(\text{NH}_4)_2\text{HPO}_4$  0.3 M solution was dripped onto a  $\text{Ca}(\text{OH})_2$  0.5 M solution suspension at  $40 \pm 2^\circ\text{C}$  with a flow rate of 1.3 mL per minute for approximately 1 hour, adding 30% gelatin solution and 2 grams of PVA. The dripping process was carried out while continuously stirring with a magnetic stirrer. The reaction produces the base  $\text{NH}_4\text{OH}$ , so the pH must be adjusted to 10 by adding ammonium hydroxide solution and checking the pH every minute. The synthesised mixture was then decanted for 24 hours and followed by sonication for 6 hours. After that, the solution was centrifuged for 15 minutes at 4500 rpm. The pellet obtained was filtered using a vacuum dryer and rinsed with distilled water. The resulting precipitate was then dried in an oven at  $100^\circ\text{C}$  for 3 hours. After drying, the precipitate was finely ground and heated in a furnace at  $1000^\circ\text{C}$  for 3 hours. The formed HAp-gelatin-PVA powder was removed and left at room temperature. The HAp-gelatin-PVA powder was then characterised using XRD and FTIR spectrophotometer.

### Nanotube Formation on the Surface of Ti-6Al-4V Metal Alloy (Charlena *et al.* 2022)

The Ti-6Al-4V metal alloy was cut to a diameter of 14 mm with a thickness of 5 mm. The metal alloy pieces were buffed using SiC paper or 320-1500 grit sandpaper. Next, the metal was ultrasonically cleaned with ethanol, acetone and distilled water (sonication) for 15 minutes each. The Ti-6Al-4V pieces were removed, rinsed with distilled water, and dried at room temperature. The anodisation method was used to form nanotubes on the surface of a metal. The Ti-6Al-4V pieces were anodised in ethylene glycol-aqueous solution (9:1) containing 0.6%  $\text{NH}_4\text{F}$  at a voltage of 20 V from direct current (DC) for 3 hours. The anodisation process was carried out with two electrodes: platinum (Pt) electrode as the cathode (negative pole) and Ti-6Al-4V piece as the anode (positive pole). The distance between the cathode and anode was made to be 4 cm. After the anodisation process, the Ti-6Al-4V pieces were removed, rinsed with distilled water, and dried at room temperature. The anodised metal was characterised by SEM.

### Coating with Dip-Coating Method

HAp-gelatin-PVA composite weighed as much as 2 g and dissolved in 20 mL of 96% ethanol. After that, the metal was immersed in the HAp-gelatin-PVA composite solution with a soaking time of one week until the ethanol evaporated. Then, the metal was lifted vertically slowly and dried at room temperature. After drying, the metal coated with HAp-gelatin-PVA composite was analysed using SEM, XRD, corrosion resistance test, and in vitro test on SBF solution.

### Corrosion Resistance Test (Charlena *et al.* 2022)

The Ti-6Al-4V metal alloy was cut into equal sizes and shaped into a round to a diameter of 14 mm. The sample was assembled on the working electrode, and then three electrodes as corrosion test instruments were dipped into a flask containing a 600 mL 0.9% NaCl infusion solution corrosion medium. The standard calomel electrode was used as the comparison electrode, two carbon rods were used as auxiliary electrodes, and Ti-6Al-4V metal alloy was used as the working electrode. The corrosion cell was connected to a potentiostat/galvanostat model 273 device at a potential of -20 mV to 20 mV. Corrosion resistance tests were conducted on Ti-6Al-4V metal alloy, Ti-6Al-4V nanotube metal alloy, Ti-6Al-4V nanotube metal alloy and non-nanotube clad composite.

### In Vitro test on SBF solution (Charlena *et al.* 2022)

The 1000 ppm Ca primer standard solution was diluted to 100 ppm into a 100 mL volumetric flask. The 100 ppm Ca primer standard solution was used to make a series of Ca standards with concentrations of 2, 4, 8, 12, and 16 ppm. The standard solution was made by pipetting 100 ppm Ca parent standard solution as much as 1, 2, 4, 6, and 8 mL and transferred into a 50 mL volumetric flask and adjusted to the limit. The standard solution was measured using AAS with a wavelength of 422.7 nm. Furthermore, Ti-6Al-4V nanotube and non-nanotube metal alloys have been coated composite immersed in

SBF solution for 14 days. The soaking results were taken every day 1, 5, 7, 9, 11, and 14 as much as 10 mL. After that, the calcium content was measured using AAS at a wavelength of 422.7 nm.

## RESULTS AND DISCUSSION

### HAp-Gelatin-PVA Composite

HAp is a ceramic biomaterial that belongs to the calcium phosphate group and has a mineral composition similar to bone tissue. HAp is a calcium phosphate compound that has the molecular formula  $\text{Ca}_{10}(\text{PO}_4)_6(\text{OH})_2$  with a Ca/P ratio of approximately 1.67. HAp can accelerate the growth of new bone directly bonded to bone tissue chemically through the formation of apatite layer biologically by interfacial bonding (Mahabole *et al.* 2012). An important requirement for a biomaterial to bind directly to living bone is that it can form an apatite layer on its surface when implanted in the body. The characteristic peak of HAp appears at  $2\theta$  31.79°-33.88°. HAp synthesised from spotted leopard shells also shows a peak at about 25.65° (Charlena *et al.* 2018b).

The diffractogram of HAp was obtained by the wet precipitation method as seen in Figure 1. XRD analysis aims to identify the mineral phase of HAp and is characterised by the appearance of X-ray diffraction patterns at  $2\theta$  angles of 20-80°. Typical X-ray diffraction patterns of the synthesised HAp were observed at  $2\theta$  angles, namely 26.05°, 31.96°, 33.09°, 32.03°, 34.24°, 40.00°, 46.87°, 48.21°, 49.63°, 50.65°, 51.44°, 52.26°, 53.33°, and 56.00°. The X-ray diffraction patterns obtained showed peaks corresponding to the characteristic peaks of HAp. These results are not much different from the results of Shirdar *et al.* (2016), who reported that the synthesised HAp was observed at angles  $2\theta$  (°): 23, 25, 28, 31, 32, 33, 35.5, 47, 49.5, 51, 52, 53, 54, and 56. HAp mineral phase was also identified by comparing the HAp spectrum data obtained with JCPDS HAp data number 09-0432. The spectrum results obtained show that the hydroxyapatite mineral phase has been formed.

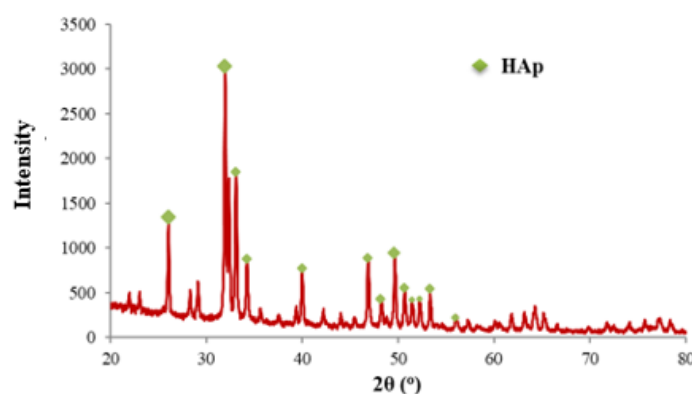


Figure 1. XRD diffractogram of HAp

Gelatin is a natural biopolymer in the form of collagen-derived protein. Gelatin is biocompatible and osteoconductive, fulfilling the requirements for use as a bone implant (Monica *et al.* 2016). Polyvinyl alcohol (PVA) is a polymer that has hydrophilic properties and is an adhesive. PVA is widely used to replace damaged or diseased body tissues because it has physicochemical properties, especially excellent biotribological properties, such as smooth surfaces, friction resistance, and wear. PVA has mechanical characteristics and biocompatibility that can be used to improve composite capabilities (Maruf *et al.* 2013).

Composites of HAp-gelatin-PVA have been developed as suitable materials for repairing hard tissues due to their similar composition to the hard tissue itself, good biocompatibility, and high osteoconductive activity. Pure gelatin has a typical X-ray diffraction pattern at a  $2\theta$  angle of  $20^\circ$  (Karthika *et al.* 2015), while PVA's X-ray diffraction pattern is typical at a  $2\theta$  angle of  $19.8^\circ$  (Wang *et al.* 2010). The X-ray diffraction patterns of gelatin and PVA do not appear because both compounds are organic compounds, and their structures are not crystalline (Wang *et al.* 2010). The diffractogram of HAp-gelatin-PVA composite synthesised by the in-situ wet precipitation method can be seen in Figure 2 and identified with the help of HAp XRD data based on JCPDS number 09-0432. X-ray diffraction patterns of HAp were observed at angles  $2\theta$  ( $^\circ$ ): 25.82, 31.73, 32.14, 32.87, 34.02, 39.76, 46.67, 49.44, 50.46, 51.24, 52.05, and 53.14. These results are not much different from the results of research by Kartikha *et al.* (2015), the HAp spectrum was

observed at angles  $2\theta$  ( $^\circ$ ): 25.83, 31.54, 32.28, 32.80, 34.06, 39.89, 46.69, 48.27, 49.26, 50.42, 52.11, and 53.11. This shows that gelatin concentration has no effect on the angle of HAp (Karthika *et al.* 2015), as well as the addition of PVA.

### Functional Group Analysis of HAp and HAp-Gelatin-PVA Composite

In addition to diffraction patterns, the functional groups of HAp without gelatin-PVA and HAp-gelatin-PVA composites that has been synthesised were also analysed by FTIR. FTIR characterisation has been carried out to identify the functional groups of HAp and HAp-gelatin-PVA composite. The composite FTIR characterisation results also confirmed that the composite coated with the Ti-6Al-4V metal alloy was a HAp-gelatin-PVA composite. Characteristic bands of HAp can be observed through the presence of splitting bands at wave numbers (in  $\text{cm}^{-1}$ ) around 600, around 962, and around 1049-1030, indicating P-O stretching and bending vibrations of the phosphate group, as well as around 3569, indicating hydroxyl group stretching vibrations. Absorption bands were also observed at wave numbers 1300-1650, indicating the stretching and bending vibrations of the C-O bond in the  $(\text{CO}_3)^{2-}$  ion (Charlena *et al.* 2023).

FTIR spectra produce typical absorption peaks at wave numbers with specific intensities. Functional groups that characterise the presence of HAp compounds are indicated by the appearance of peaks at wave numbers  $4000\text{-}400\text{ cm}^{-1}$ . Based on the FTIR spectrum of HAp obtained (Figure 3), it shows

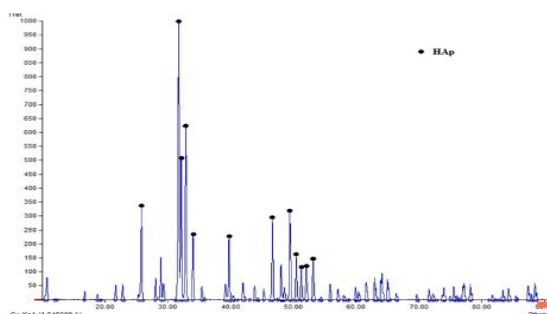


**Figure 2.** X-ray diffractogram of in-situ HAp-gelatin-PVA powder

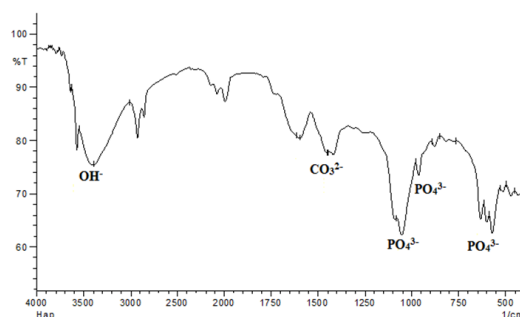


**Figure 3.** FTIR spectrum of HAp



vibrational absorption bands at wave numbers (in  $\text{cm}^{-1}$ ): 3383.14 indicating OH-stretching vibrations, 1053.13 indicating  $\text{PO}_4^{3-}$  asymmetric stretching vibrations, 962.48 and 877.61 indicating  $\text{PO}_4^{3-}$  symmetry stretching vibrations, 630.72 and 569 indicating  $\text{PO}_4^{3-}$  asymmetry bending vibrations, and 1448.54 indicating  $\text{CO}_3^{2-}$  vibrations. The  $\text{PO}_4^{3-}$  and OH absorptions are characteristic of HAp. The  $\text{CO}_3^{2-}$  vibration indicates that  $\text{CaCO}_3$  still remains in the HAp powder. According to Monica *et al.* (2016),  $\text{CO}_3^{2-}$  can substitute  $\text{PO}_4^{3-}$  in the HAp lattice to form carbonate apatite types A and B or AKA and AKB.

According to Monica *et al.* (2016), the absorption bands of pure gelatin are indicated by the presence of amide group absorption bands. The absorption bands of amide A, amide I, amide II, and amide III vibrations are observed at wave numbers (in  $\text{cm}^{-1}$ ): 3419 N-H stretching vibrations, 1659 C=O stretching vibrations, 1537 N-H bending vibrations, and 1240 C-N stretching vibrations. The absorption bands of pure PVA were observed at wave numbers (in  $\text{cm}^{-1}$ ): C-H stretching and bending vibrations at wave numbers 2945 and 1337, C-C stretching vibrations at 854, O-H stretching vibrations at 332, C-O stretching vibrations at 1098, and CH-OH bending vibrations 1427. The altered amide group absorption bands indicate that inorganic-organic bonding ( $\text{Ca}^{2+}\text{-COO}^-$ ) has occurred in the form of HAp-gelatin composites. The altered amide group absorption bands also indicate that hydrogen bonding ( $\text{OH}\cdots\text{NH}$ ) has been formed from the OH group on PVA with the NH group of gelatin.

The FTIR spectrum of in-situ HAp-gelatin-PVA in Figure 4 shows the absorption bands of OH- and N-H stretcher vibrations at wave numbers (in  $\text{cm}^{-1}$ ): 3570.24 and 3435.22,  $\text{PO}_4^{3-}$  asymmetry stretching vibrations at 1056.99,  $\text{PO}_4^{3-}$  symmetry stretching vibrations at 960.55 and 877.61, and  $\text{PO}_4^{3-}$  asymmetry bending vibrations at 632.65 and 570.9, and 1458.18 indicating  $\text{CO}_3^{2-}$  vibrations. In addition, there are gelatin vibrational absorption bands in the form of amino acid polymers with the main functional groups C=O and N-H. This can be seen from the transmittance intensity of the OH-stretching vibration, which is slightly smaller, or the absorption is slightly larger due to the OH absorption band

overlapping with the N-H absorption band of gelatin. The C=O absorption band of amino acids derived from gelatin amino acids was observed at 1761.87  $\text{cm}^{-1}$ . According to Bilton *et al.* (2012), the OH absorption on HAp is small and does not widen because the OH formed is in the HAp crystal, so it is more rigid and difficult to vibrate. Meanwhile, according to Hossan *et al.* (2014), the absorption at wave number 1328  $\text{cm}^{-1}$  effectively confirms the chemical bond formed between the carboxyl group in gelatin and the HAp phase.

Based on the FTIR spectrum in Figure 4, many of the expected absorption bands did not appear. The absorption bands that do not appear are amide II and amide III, which can indicate the presence of gelatin and absorption bands that can indicate the presence of PVA. This is possible due to the high sintering temperature used during the in-situ synthesis of HAp-gelatin-PVA composites, which is 1000°C. This also indicates that the synthesised HAp-gelatin-PVA composite has poor purity.

### Nanotube Formation of Ti-6Al-4V Metal Alloy

Ti-6Al-4V metal alloys are widely used in biomedical applications due to their biocompatibility, biomechanical properties and corrosion resistance (Narayanan *et al.* 2011). However, it lacks the bioactive properties to induce calcium phosphate (CaP) precipitation upon implantation in the body, which can reduce the osseointegration of bone with the implant material (Liu *et al.* 2012). Surface modifications can be made to reduce this effect by coating metals with bioactive materials or materials with rough surfaces (Kuroda & Okido 2011). One way to do this is by forming nanotubes on the surface of Ti-6Al-4V metal alloy by the anodisation method. Nanotubes are a form of a compound composition that has a tube-like morphology and nanoparticle-sized pores.

Anodisation is the formation of a thin oxide film on the surface of a metal/workpiece by electrolysis to thicken or strengthen the natural protective layer of the metal. The principle of anodisation, the electrolysis cell, essentially converts electrical energy into a chemical reaction. This process uses two electrodes, the cathode and the anode (Figure 5).

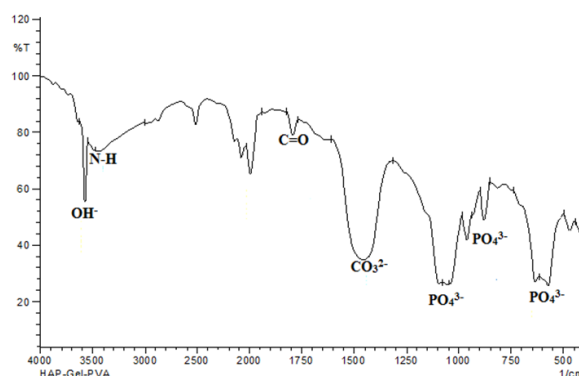


**Figure 4.** FTIR spectrum of in-situ HAp-gelatin-PVA

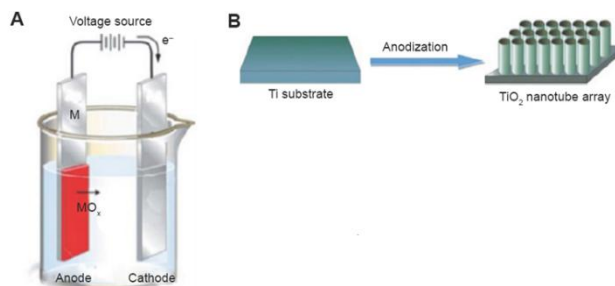


**Figure 5.** Illustration of the anodization process (Wang *et al.* 2016)

Pt metal is used as the cathode or inert materials such as carbon (C) and Au, while Ti-6Al-4V metal alloy is used as the anode. The Ti-6Al-4V metal alloy can spontaneously form a titanium oxide (TiO<sub>2</sub>) layer on its surface. The formation of this layer can occur in both air and electrolyte environments. The process of forming a TiO<sub>2</sub> nanotube layer was carried out in this study, namely, using an electrolyte solution. This process must use an electrolyte solution containing F<sup>-</sup> ions. Liu *et al.* (2012) used NaF, NH<sub>4</sub>F, and HF solutions. Meanwhile, in this study, the electrolyte solution used was NH<sub>4</sub>F.

Minagar *et al.* (2012) state that the mechanism of nanotube formation by anodisation method occurs in three stages. In the first stage, the cathode will undergo a reduction reaction so that H<sub>2</sub> gas will be formed. In the second stage, the anode will undergo an oxidation reaction to form an oxide layer. The oxidising metal species will react with O<sup>2-</sup> ions (from H<sub>2</sub>O) to form the oxide layer. Ti metal has a high reactivity to O<sub>2</sub>, resulting in a stable oxide layer. Finally, the oxide layer will undergo chemical dissolution in an electrolyte solution containing F<sup>-</sup> ions to form soluble fluoride complex compounds. This is an important stage in the formation of nanotubes. Chemical dissolution reactions dominate at the beginning of anodisation, resulting in small holes that act as nuclei in pore formation. Pores and voids appear on the surface of the oxide layer. This is the first step in forming nanotubes, and the high acidity at the base of the tube helps the pores form a tube structure (Figure 6).

Anodisation was carried out for 3 hours at a voltage of 20 V using DC current. With a DC current, the electricity carried by F<sup>-</sup> ions in the electrolyte solution will move unidirectionally, which has direct implications for forming small holes that act as the core in forming pores before nanotubes are formed. Robin *et al.* (2014) successfully formed TiO<sub>2</sub> nanotubes using 1% NH<sub>4</sub>F solution for 2 hours at 20 V voltage. Other studies, such as Vera-Jiménez *et al.* (2015), successfully formed nanotubes with a concentration of F<sup>-</sup> ions in the electrolyte solution below 5% but using a high voltage for 11.5 hours. If the concentration of F<sup>-</sup> ions is below 5%, the solution must be combined with an organic solution, such as glycerol or ethylene glycol (Vera-Jiménez *et al.* 2015). The viscosity of ethylene glycol can affect the growth rate and length of nanotubes, maintain the

thickness of the oxide layer at the bottom of the tube, and facilitate ionic migration (Regonini *et al.* 2013).

The results of SEM (Figure 7) show that the TiO<sub>2</sub> nanotubes obtained are more homogeneous and uniform after anodisation with ethylene glycol-H<sub>2</sub>O (9:1 v/v) electrolyte solution containing 0.6% NH<sub>4</sub>F at room temperature. The diameter of the nanotubes formed in this study is about 30-40 nm. This is in line with the research of Minagar *et al.* 2012 which reported that nanotubes will form when the potential is around 30-120V, and using ethylene glycol, organic electrolyte solution will have a diameter of around 20-160nm. However, Figure 7a still shows some parts that are not entirely formed nanotubes. This could be due to factors affecting the anodisation process: F<sup>-</sup> ion concentration, electrolyte type, anodisation potential, and anodisation time (Regonini *et al.* 2013).

### Coating of Ti-6Al-4V Metal Alloy with HAp-Gelatin-PVA Composite

HAp is a biomaterial with good biocompatibility but is brittle when implanted in a living body. The preparation of HAp-gelatin-PVA composite aims to improve the brittle nature and increase the mechanical strength of HAp. During the formation process of the HAp-gelatin composite, Ca<sup>2+</sup> ions will form covalent bonds with R-COO<sup>-</sup> ions on gelatin molecules. The bond will induce a shortening of the distance between HAp-gelatin fibrils (Hossan *et al.* 2014). In this study, the preparation of HAp-gelatin-PVA composites was carried out in situ. The 30% HAp-gelatin composite was chosen because it had the highest crystallinity, and SEM results showed smaller and more homogeneous granules (Monica *et al.* 2016). Charlena *et al.* (2022) reported that the added PVA will form a smoother composite microstructure.

Coating Ti-6Al-4V metal alloy with HAp-gelatin-PVA composite using the dip-coating method. The dip-coating method can produce a coating thickness of 0.05-0.5 mm. The advantages of this method include the uniformity of the HAp surface, which can be adjusted, the time required is fast, and the composite layer is deposited on the metal surface without any reaction or decomposition occurring between the composite and the metal surface (Mohseni *et al.* 2014). In this study, nanotube and non-nanotube Ti-6Al-4V metal alloys were coated to compare the coating results. The metal alloy was

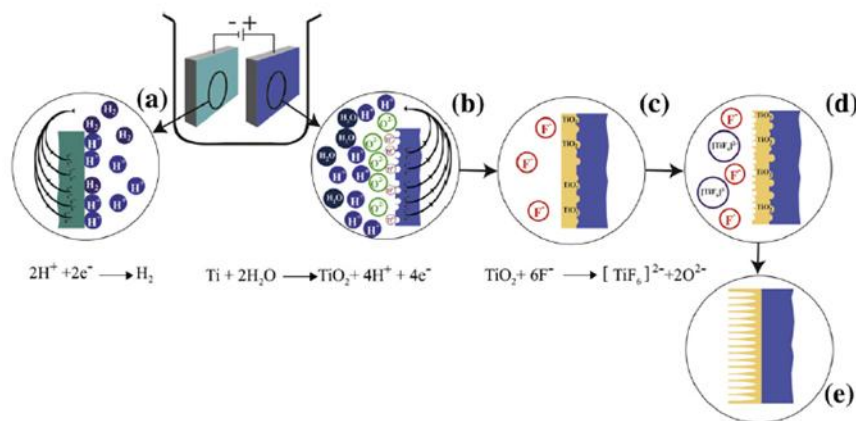


**Figure 6.** Mechanism of TiO<sub>2</sub> nanotube formation: (a) cathodic reaction, (b) anodic reaction, (c) transition state of TiO<sub>2</sub> layer, (d) nanotube formation, and (e) TiO<sub>2</sub> nanotube. (Minagar *et al.* 2012)

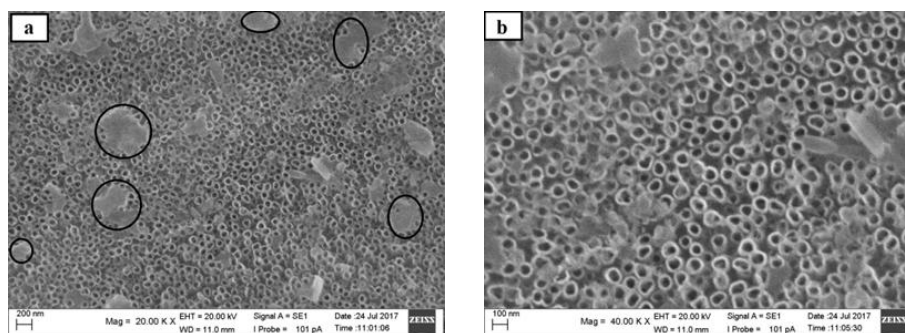


**Figure 7.** (a) Surface morphology of Ti-6Al-4V alloy nanotubes at 20000x magnification, (b) Ti-6Al-4V alloy nanotubes at 40000x magnification

immersed in HAp-gelatin-PVA composite, dissolved in ethanol for 7 days, and lifted vertically slowly.

Based on the coating results, nanotube and non-nanotube metal alloys were successfully coated by HAp-gelatin-PVA composite. Identification of the coating results on both metal alloys can be observed with the naked eye. The nanotube metal is evenly coated on the entire metal surface and is thicker than the non-nanotube metal (Figure 8). However, to determine the best results, it is necessary to characterize using SEM and XRD to determine the morphology and ensure that the mixing process of HAp and gelatin-PVA does not form new compounds.

SEM characterized the coating results on the surface and transverse surface to determine the morphology of the HAp-gelatin-PVA composite, composite particle size and pore size. HAp-gelatin-PVA coated on Ti-6Al-4V nanotube and non-nanotube metal alloys were characterized on the surface and transverse surface where HAp-gelatin-PVA was attached to the metal alloy (Figure 9 a, b, c, and d). Based on the SEM results, it can be seen that the morphology of Ti-6Al-4V-HAp-gelatin-PVA is in the form of smaller and homogeneous granules because the presence of gelatin strengthens the HAp bond (Zandi *et al.* 2009) so that the HAp molecules

become more organized, relatively the same size, and more homogeneous. Particle sizes observed in nanotube and non nanotube metal alloys are in the range of 100-200 nm and 200-300 nm, respectively. The observed pores have sizes ranging from 400-450 nm and 850-900 nm, which are pores formed in nanotube and non nanotube metal alloys, respectively. This indicates that the dressing particles are more well distributed on the surface of the nanotube metal alloy. Particles with large sizes can reduce the strength of the material.

In addition to SEM characterization, the alloys were also characterized by XRD to ensure that the HAp-gelatin-PVA mixing process did not form new compounds. Figure 10 shows that the alloying of Ti-6Al-4V non-nanotubes and nanotubes with HAp-gelatin-PVA did not shift the  $2\theta$  angle too much. The main peaks in non-nanotube metal were observed at  $2\theta(^{\circ})$  25.99, 31.98, 32.00, and 32.03, while nanotube metal was observed at  $2\theta(^{\circ})$  25.75, 31.72, 32.82, 32.87, and 49.44 which shows the characteristics of HAp. The addition of gelatin concentration has no effect on the angle of HAp (Karthika *et al.* 2015) and the addition of PVA. X-ray diffraction pattern of Ti also appeared in the diffractogram. Based on identification with JCPDS Ti data number 44-1294,



**Figure 8.** Ti-6Al-4V metal alloy after sheathing (a) nanotubes and (b) non nanotubes

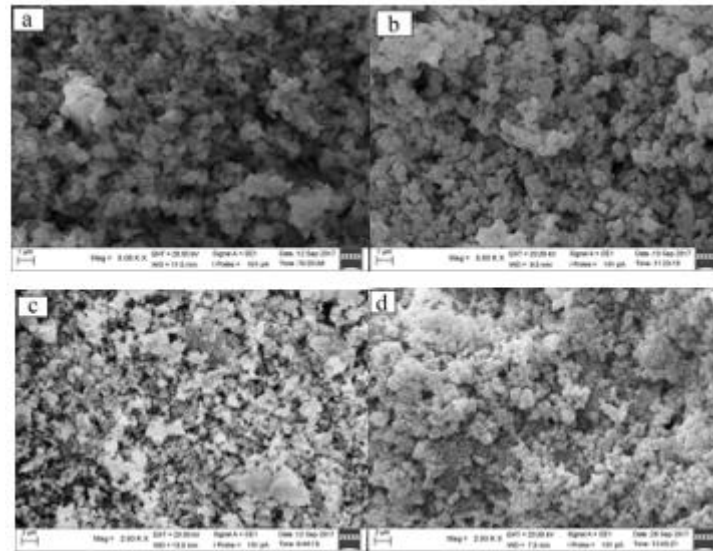


**Figure 9.** Morphology of HAp-gelatin-PVA composite on the surface and cross section of nanotubes (a) (b) and non nanotubes (c) (d)

the characteristic peak of titanium was observed at  $2\theta$   $40.54^\circ$  in both non-nanotube and nanotube metals.

#### Ca<sup>2+</sup> Ion Release in Physiological Solution

Ti-6Al-4V nanotube and non-nanotube metal alloys coated with HAp-gelatin-PVA composite were immersed in a physiological solution for 14 days to observe the release of Ca<sup>2+</sup> ions from HAp or the binding of Ca<sup>2+</sup> ions from the physiological solution. The physiological solution used was simulated body fluid (SBF), which contains the same ions as human body fluids. Calcium concentration during immersion was observed on days 1, 3, 5, 7, 9, 11, and 14 using AAS. The rate of Ca<sup>2+</sup> ion release from HAp was proportional to the rate of increase in calcium concentration in the SBF solution. The rate of increase of Ca<sup>2+</sup> ion concentration in SBF solution is shown in Figure 11.

Ca<sup>2+</sup> concentration data obtained from AAS showed a decrease in concentration on day 14 (Figure 11). This indicates that there will be a process of precipitation of Ca<sup>2+</sup> ions towards apatite crystals. Charlena *et al.* (2022) stated that the first step in the growth of apatite crystals is seen after seven days of immersion because, in that period, Ca<sup>2+</sup> precipitation

occurs. Precipitated Ca can stimulate nucleation and accelerate the process of new bone growth. Jamil *et al.* (2015) stated that a solution saturated with Ca<sup>2+</sup> ions will also attract phosphate ions and form calcium phosphate, accelerating the calcium phosphate precipitation process. According to Mohandes *et al.* (2014), the decrease in Ca<sup>2+</sup> ion concentration occurs on the 3rd day of immersion, while in this study, until the 11th day of immersion, there was no decrease in Ca<sup>2+</sup> ion concentration. This is due to the presence of gelatin in the composite and a layer of TiO<sub>2</sub> nanotubes on the surface of the Ti-6Al-4V metal alloy that can withstand the release of Ca<sup>2+</sup> ions into the SBF solution.

#### Corrosion Rate of Ti-6Al-4V Metal Alloys Before and After HAp-Gelatin-PVA Coating

The corrosion process due to body fluids that occur on metal implants will cause inflammation and produce toxic ions that are harmful to the body. The corrosion resistance test aims to determine the compatible properties of Ti-6Al-4V metal alloy before coating and after coating with HAp-gelatin-PVA composite. Marin *et al.* (2011) reported that



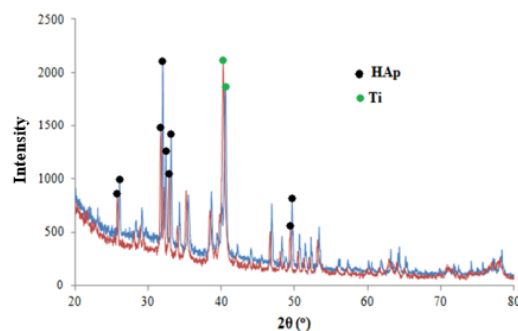


**Figure 10.** X-ray diffractograms of Ti-6Al-4V non nanotube-HAp-gelatin-PVA (blue) and Ti-6Al-4V nanotube-HAp-gelatin-PVA (red)

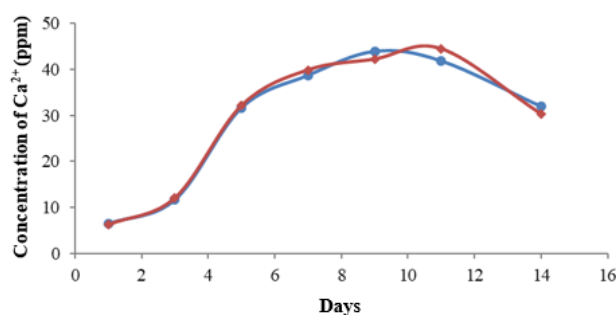


**Figure 11.** Ca<sup>2+</sup> concentration curve of Ti-6Al-4V nanotube metal alloy (blue) and Ti-6Al-4V non nanotube (red) after soaking for 14 days.

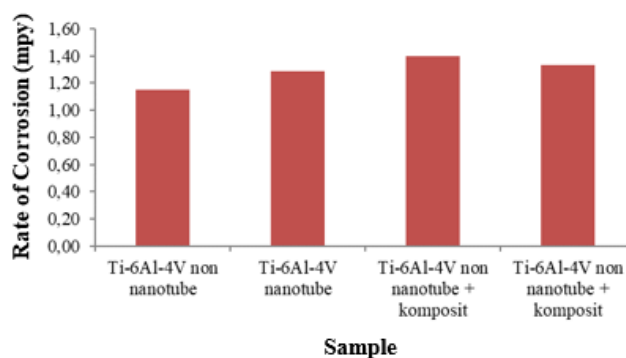


**Figure 12.** Corrosion rate of Ti-6Al-4V alloy

Titanium (Ti) and its alloys are widely used as dental and orthopaedic implants because they have good mechanical properties, low cytotoxicity, corrosion resistance, and biocompatibility. High corrosion resistance is one of the main requirements for a metal implant to have a long life in the body. Nanotube formation and HAp-gelatin-PVA composite coating on Ti-6Al-4V metal alloy is one way to improve the corrosion resistance of the metal.

The corrosion rate was measured by conditioning the metal alloy before and after being coated with HAp-gelatin-PVA composite as an implant in the body that will be in direct contact with the body fluid medium. A 0.9% NaCl solution was used as the corroding medium because it is similar to body fluids. The corrosion test results in Figure 12 show

that the corrosion rate of Ti-6Al-4V nanotube metal alloy before and after the coating is 1.29 mpy and 1.33 mpy, respectively. Meanwhile, the corrosion rate of Ti-6Al-4V non-nanotube metal alloy before and after sheathing was 1.15 mpy and 1.4 mpy. The Ti-6Al-4V metal alloy after composite coating has a higher corrosion rate than before composite coating. This is possible because the composite layer covering the metal alloy is too thin, increasing the corrosion rate. Sari *et al.* (2015) obtained the results of a 316L stainless steel metal corrosion rate of 4,872 mpy in their research. Bhola *et al.* (2011) stated that in titanium metal, under entirely passive conditions, the corrosion rate is less than 0.8 mpy (0.02 mmpy) and has a maximum corrosion rate of 5 mpy (0.13 mmpy), which is acceptable for biomaterial

application design. It is shown that the metal alloy Ti-6Al-4V nanotube and non-nanotube encapsulated HAp-gelatin-PVA composite has a better corrosion rate compared with 316L stainless steel metal.

## CONCLUSION

Nanotube formation on Ti-6Al-4V metal alloy has been successfully carried out using ethylene glycol-water electrolyte solution in the ratio of 9:1 (0.6%  $\text{NH}_4\text{F}$ , 20 V, 3 hours). SEM characterization results show that the nanotube hole diameter is about 30-40 nm and formed homogeneously. The result of coating metal nanotube alloy with HAp-gelatin-PVA composite is even and thicker. The morphology of the dressing composite is homogeneous small granules. XRD characterization shows that the HAp-gelatin-PVA composite with coated nanotube metal alloy has a smaller crystal size. Nanotube formation and coating with HAp-gelatin-PVA composite has poor bioactivity and does not improve the corrosion resistance of Ti-6Al-4V metal alloy.

## REFERENCES

- Bhola, R., Bhola, S. M., Mishra, B. & Olson, D. L. (2011). Corrosion in titanium dental implants/prostheses—a review. *Trends Biomater Artif Organs*. **25**(1): 34-46.
- Bilton M, Milne S.J., Brown A.P. (2012). Comparison of hydrothermal and sol-gel synthesis of nano-particulate hydroxyapatite by characterization at the bulk and particle level. *Open Journal of Inorganic Non-metallic Materials*. **2**(1). 1-10.
- Charlena, C., Suparto I.H., Laia D.P.O. (2023). Synthesis and characterization of hydroxyapatite from *Polymesoda placans* shell using wet precipitation method. *Jurnal Bios Logos*. **13**(1): 71-82.
- Charlena, C., Kemala, T. & Ravena, R. (2022). Coating of nanotube Ti-6Al-4V alloy with hydroxyapatite-chitosan-polyvinyl alcohol composite. *IJFAC (Indonesian Journal of Fundamental and Applied Chemistry)*. **7**(2): 58-67.
- Charlena, C., Kemala, T. & Wulanawati, A. (2018a). Utilization of electrolyte solution in nanotube formation on Ti-6Al-4V metal alloy. *IJFAC (Indonesian Journal of Fundamental and Applied Chemistry)*. **3**(1): 1-6.
- Charlena, Bikharudin A. Wahyudi S.T. (2018b). Synthesis and characterization of hydroxyapatite-collagen-chitosan (HA/Col/Chi) composite coated on Ti6Al4V. In *IOP Conference Series: Materials Science and Engineering*. **299**(1): 012028.
- Chen, Q. & Thouas, G. A. (2015). Metallic implant biomaterials. *Materials Science and Engineering: R: Reports*. **87**: 1-57.
- Hossan M.J., Gafur M.A., Kadir M.R. & Karim M.M. (2014). Preparation and characterization of gelatin-hydroxyapatite composite for bone tissue engineering. *International Journal of Engineering & Technology IJET-IJENS*. **12**(1): 24-32.
- Jamil, M., Abida, F., Hatim, Z., Ellassfour, M. & Gourri, E. (2015). Effects of ions traces on the dissolution of bioceramics composed of hydroxyapatite and  $\beta$ -tricalcium phosphate. *Mediterranean Journal of Chemistry*. **4**(1): 51-58.
- Karthika, A., Kavitha, L., Surendiran, M., Kannan, S. & Gopi, D. (2015). Retracted Article: Fabrication of divalent ion substituted hydroxyapatite/gelatin nanocomposite coating on electron beam treated titanium: mechanical, anticorrosive, antibacterial and bioactive evaluations. *Rsc Advances*. **5**(59): 47341-47352.
- Kuroda, K. & Okido, M. (2012). Hydroxyapatite coating of titanium implants using hydroprocessing and evaluation of their osteoconductivity. *Bioinorganic chemistry and applications*. **2012**(1): 730693.
- Liu, C.L., Wang, Y.J., Wang, M., Huang, W.J. & Chu, P.K. (2012). Electrochemical behaviour of  $\text{TiO}_2$  nanotube on titanium in artificial saliva containing bovine serum albumin. *Corrosion Engineering, Science and Technology*. **47**(3): 167-169.
- Marin, C., Bonfante, E.A., Granato, R., Suzuki, M., Granjeiro, J.M. & Coelho, P. G. (2011). The effect of alterations on resorbable blasting media processed implant surfaces on early bone healing: a study in rabbits. *Implant Dentistry*. **20**(2): 167-177.
- Maruf, S.H., Wang, L., Greenberg, A.R., Pellegrino, J. & Ding, Y. (2013). Use of nanoimprinted surface patterns to mitigate colloidal deposition on ultrafiltration membranes. *Journal of Membrane Science*. **428**: 598-607.
- Mahabole, M.P., Bahir, M.M., Kalyankar, N.V. & Khairnar, R.S. (2012). Effect of incubation in simulated body fluid on dielectric and photoluminescence properties of nano-hydroxyapatite ceramic doped with strontium ions. *Journal of Biomedical Science and Engineering*. **5**(7): 396-405.
- Minagar, S., Berndt, C.C., Wang, J., Ivanova, E. & Wen, C. (2012). A review of the application of anodization for the fabrication of nanotubes on metal implant surfaces. *Acta Biomaterialia*. **8**(8): 2875-2888.
- Mohandes, F. & Salavati-Niasari, M. (2014). Influence of morphology on the in vitro bioactivity of hydroxyapatite nanostructures prepared by precipitation method. *New Journal of Chemistry*. **38**(9): 4501-4509.
- Mohseni, E., Zalnezhad, E. & Bushroa, A. R. (2014). Comparative investigation on the adhesion of hydroxyapatite coating on Ti-6Al-4V implant:

- A review paper. *International Journal of Adhesion and Adhesives*. **48**: 238-257.
- Monica, S., Charlena. & Suparto, I.H. (2016). Synthesis and characterization of hydroxyapatite-gelatin composites with in-situ and ex-situ wet precipitation. *Rasayan Journal Chemistry*. **9(4)**: 650-656.
- Narayanan, R., Lee, H. J., Kwon, T. Y. & Kim, K. H. (2011). Anodic TiO<sub>2</sub> nanotubes from stirred baths: hydroxyapatite growth & osteoblast responses. *Materials Chemistry and Physics*. **125(3)**: 510-517.
- Regonini, D., Bowen, C. R., Jaroenworarluck, A. & Stevens, R. (2013). A review of growth mechanism, structure and crystallinity of anodized TiO<sub>2</sub> nanotubes. *Materials Science and Engineering: R: Reports*. **74(12)**: 377-406.
- Robin, A., Ribeiro, M.B.d.A., Rosa, J.L., Nakazato, R.Z. & Silva, M.B. (2014). Formation of TiO<sub>2</sub> nanotube layer by anodization of titanium in ethylene glycol-H<sub>2</sub>O electrolyte. *Journal of Surface Engineered Materials and Advanced Technology*. **2014(4)**: 123-130.
- Sari, M., Fadli, A. & Amri, A. (2015). Pengaruh tegangan listrik dan waktu pelapisan hidroksiapatit pada logam 316L dengan metode elektroforesis deposisi (EPD). *Jurnal Online Mahasiswa FTEKNIK*. **2(2)**: 1-5.
- Shirdar, M.R., Taheri, M.M., Sudin, I., Shafaghat, A., Keyvanfar, A. & Abd. Majid, M.Z. (2016). In situ synthesis of hydroxyapatite-grafted titanium nanotube composite. *Journal of Experimental Nanoscience*. **11(10)**: 816-822.
- Vera-Jiménez, A.M., Melgoza-Alemán, R.M., Valladares-Cisneros, M. G. & Cuevas-Arteaga, C. (2015). Synthesis and mechanical/electrochemical characterization of TiO<sub>2</sub> nanotubular structures obtained at high voltage. *Journal of Nanomaterials*. **2015(1)**: 624073.
- Wang, F., Guo, E., Song, E., Zhao, P. & Liu, J. (2010). Structure and properties of bone-like-nanohydroxyapatite/gelatin/polyvinyl alcohol composites. *Advances in Bioscience and Biotechnology*. **1(03)**: 185-189.
- Wang, Q., Huang, J.Y., Li, H.Q., Chen, Z., Zhao A.Z.J., Zhang, Sun H.T., Al-Deyab S.S. & Lai Y.K. (2016). TiO<sub>2</sub> nanotube platforms for smart drug delivery: a review. *International Journal of Nanomedicine*. **11**: 4819-4834.
- Zandi, M., Mirzadeh, H., Mayer, C., Urch, H., Eslaminejad, M.B, Bagheri, F. & Mivehchi, H. (2009). Biocompatibility evaluation of nano-rod hydroxyapatite/gelatin coated with nano-HAp as a novel scaffold using mesenchymal stem cells. *Journal of Biomedical Materials Research Part A: An Official Journal of The Society for Biomaterials, The Japanese Society for Biomaterials, and The Australian Society for Biomaterials and the Korean Society for Biomaterials*. **92(4)**: 1244-1255.